

# Hyaluronate–Gold Nanorod/DR5 Antibody Complex for Noninvasive Theranosis of Skin Cancer

Hwiwon Lee,<sup>†,#</sup> Jung Ho Lee,<sup>†,#</sup> Jeosu Kim,<sup>‡</sup> Jong Hwan Mun,<sup>†</sup> Junho Chung,<sup>§</sup> Heebeom Koo,<sup>||</sup> Chulhong Kim,<sup>‡</sup> Seok Hyun Yun,<sup>||</sup> and Sei Kwang Hahn<sup>\*,†,||</sup>

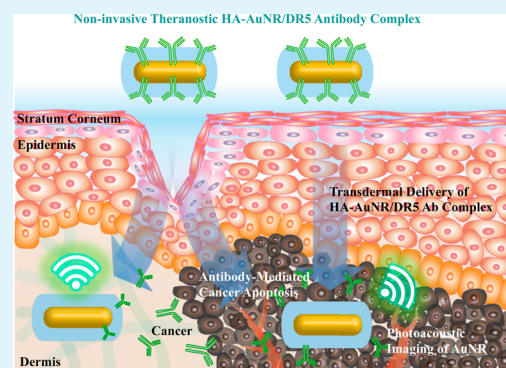
<sup>†</sup>Department of Materials Science and Engineering and <sup>‡</sup>Departments of Creative IT Engineering and Electrical Engineering, Pohang University of Science and Technology (POSTECH), 77 Cheongam-Ro, Nam-Gu, Pohang, Gyeongbuk 37673, Korea

<sup>§</sup>Department of Biochemistry and Molecular Biology and Cancer Research Institute, Seoul National University College of Medicine, Seoul 151-742 Korea

<sup>||</sup>Wellman Center for Photomedicine, Harvard Medical School and Massachusetts General Hospital, 65 Landsdowne St. UP-5, Cambridge, Massachusetts 02139, United States

**ABSTRACT:** Noninvasive transdermal delivery is a promising method with distinct advantages including patient compliance over other delivery routes. Here, hyaluronate–gold nanorod/death receptor 5 antibody (HA–AuNR/DR5 Ab) complex was developed for transdermal theranosis of skin cancer. The successful formation of the complex was corroborated by <sup>1</sup>H nuclear magnetic resonance, UV–vis spectroscopy, dynamic light scattering, zeta potential, and transmission electron microscopy. In vitro biological activity of the complex was verified by ELISA and MTT assay using HCT116 cancer cells. In addition, in vivo photoacoustic imaging and two-photon microscopy clearly visualized the transdermal delivery of HA–AuNR/DR5 Ab complex through the inevitable barrier of stratum corneum in the skin. Furthermore, in vivo antitumor effect on skin cancer model mice was confirmed from statistically significant decrease of tumor-reflecting luciferase expression levels and apoptotic signals in terminal deoxynucleotidyl transferase dUTP nick end labeling (TUNEL) assay. Taken together, we could confirm the feasibility of HA–AuNR/DR5 Ab complex as a novel theranostic platform for noninvasive transdermal treatment of skin cancers.

**KEYWORDS:** gold nanorod, hyaluronate, antibody, transdermal delivery, skin cancer



## INTRODUCTION

Gold nanoparticles (AuNPs) have been widely investigated for various biomedical applications due to their biocompatibility, simple synthesis, and facile surface modification.<sup>1</sup> AuNPs strongly interact with light depending on their environment, size, and shapes, in the forms of nanospheres,<sup>2</sup> nanorods,<sup>3</sup> nanoshells,<sup>4</sup> and nanocages.<sup>5</sup> They show unique and tunable optical-electronic properties. Remarkably, AuNPs have been used for photoacoustic bioimaging<sup>6,7</sup> and cancer hyperthermia based on their unique photothermal effect.<sup>8,9</sup> Among them, gold nanorod (AuNR) with a rodlike anisotropic morphology offers strong surface plasmon resonance (SPR) in the visible region at ca. 520 nm<sup>10</sup> and near-infrared (NIR) region,<sup>11</sup> where the light can penetrate the deep tissue area.<sup>12</sup> Furthermore, therapeutic proteins such as interferons<sup>13</sup> and antibodies<sup>14</sup> are reported to physically bind onto the surface of AuNPs by hydrophobic and electrostatic interaction.<sup>15</sup> Because of these unique properties of AuNRs, they can be exploited for various theranostic applications including biological sensing,<sup>16,17</sup> imaging,<sup>18</sup> and photothermal therapy<sup>19</sup> as well as being used as a drug delivery carrier.<sup>20</sup>

Although noninvasive transdermal drug delivery is a fascinating method with many advantages over other delivery routes, it has been available only to a limited number of drugs that are small and lipophilic due to the inevitable barrier of stratum corneum in the skin.<sup>21</sup> To enhance the transdermal drug delivery, a variety of devices have been developed including microneedles, iontophoretic systems, and ultrasound systems.<sup>21</sup> Recently, hyaluronate (HA) has been widely investigated as a promising transdermal delivery carrier of proteins and nanomaterials.<sup>22</sup> HA has been used as a skin penetration enhancer of ovalbumin,<sup>23</sup> human growth hormone,<sup>24</sup> and nano graphene oxide.<sup>25</sup> The hygroscopic HA can hydrate stratum corneum and the hydrophobic patch domain on HA chain can enhance its permeation into the skin.<sup>26</sup> Besides, HA receptors on keratinocyte and fibroblast in epidermis and dermis also facilitate the penetration and localization of HA in the skin tissue.<sup>27</sup> As an anticancer therapeutic, we exploited death receptor 5 antibody (DR5 Ab),

**Received:** September 7, 2016

**Accepted:** November 7, 2016

**Published:** November 7, 2016

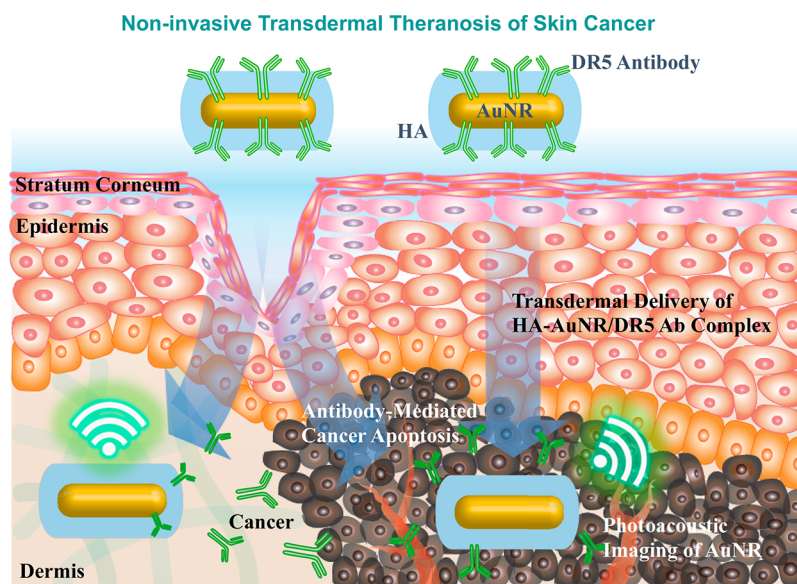


**Figure 1.** Schematic illustration for hyaluronate–gold nanorod/death receptor 5 antibody (HA-AuNR/DR5 Ab) complex for noninvasive transdermal theranosis of skin cancer.

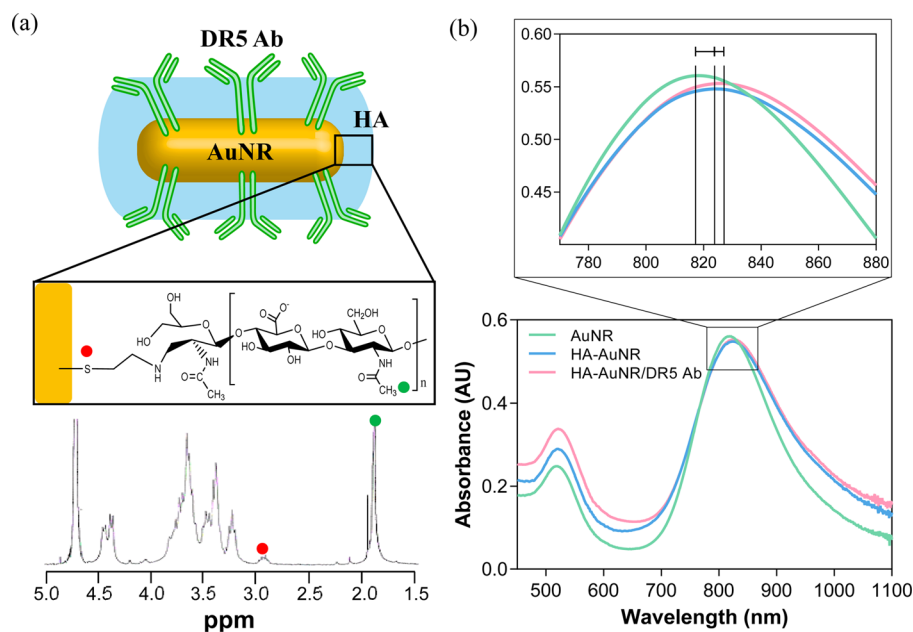


**Figure 2.** (a)  $^1\text{H}$  NMR of end-group thiolated HA (HA-SH) in HA-AuNR/DR5 Ab complex. (b) UV–vis spectra of AuNR, HA-AuNR, and HA-AuNR/DR5 Ab complex.

which specifically targets death receptor 5 (DR5) and is highly expressed on cancer cell membrane, to induce apoptosis of cancer cells.<sup>28</sup> DR5 belongs to a tumor necrosis factor (TNF)-receptor superfamily that binds TNF-related apoptosis-inducing ligand (TRAIL) and has been investigated as a target receptor for cancer therapy.<sup>29</sup>

In this work, we developed a versatile theranostic platform of HA-AuNR/DR5 Ab complex for photoacoustic imaging and antibody cancer therapy after its noninvasive transdermal delivery. The conjugation of negatively charged HA on the surface of AuNR can highly improve the stability of HA-AuNR/DR5 Ab complex, preventing the nonspecific interaction between AuNRs and serum protein in the body.<sup>14</sup> AuNR absorbing NIR lasers can be harnessed as a photoacoustic imaging platform for diagnostic applications. In addition, HA-

coated AuNR can serve as a transdermal nanocarrier of DR5 Ab for the treatment of skin cancer. In combination, HA-AuNR/DR5 Ab complex was assessed for noninvasive theranosis of skin cancer.

## RESULTS AND DISCUSSION

**Preparation and Characterization of HA-AuNR/DR5 Ab Complex.** Figure 1 shows a schematic illustration of noninvasive transdermal theranostic system of HA-AuNR/DR5 Ab complex for the treatment of skin cancer. AuNR was prepared as both an imaging agent and a transdermal drug delivery carrier by the seed-mediated growth using cetyltrimonium bromide (CTAB).<sup>30</sup> HA was chemically modified to introduce thiol groups at the end of HA chains and attached on

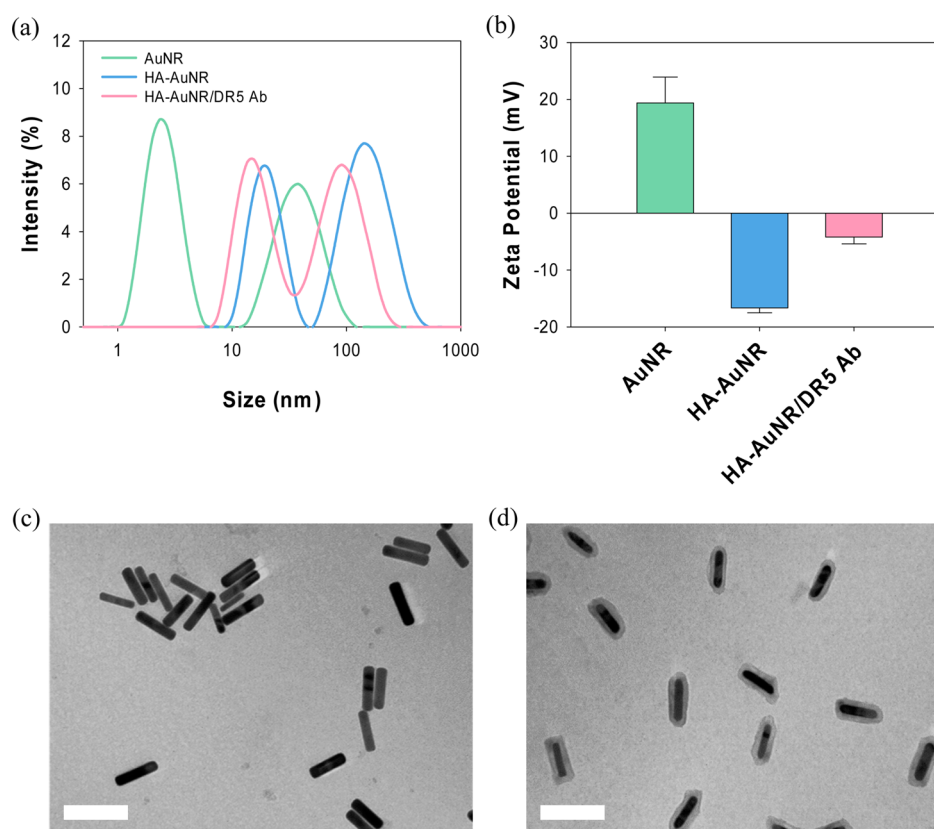


**Figure 3.** DLS for (a) hydrodynamic diameters and (b) zeta potentials of AuNR, HA-AuNR, and HA-AuNR/DR5 Ab complex. TEM images of (c) HA-AuNR and (d) HA-AuNR/DR5 Ab complex (scale bar = 100 nm).

the surface of AuNRs via gold–thiol chemistry.<sup>31</sup> HA stabilizes the complex even in the serum and facilitates the penetration of drugs through the skin. Considering the size of antibody (ca. 10 nm) and AuNR (ca. 38 nm), 10 kDa of HA (ca. 25 nm) was selected to be adequate to prepare the compact complex for transdermal delivery.<sup>13,32</sup> The successful synthesis of end-thiolated HA (HA-SH) was confirmed from the peak at 2.9 ppm of <sup>1</sup>H NMR (Figure 2a) and Ellman's assay, which revealed more than 90% thiol modification of HA chains. After that, humanized IgG1 monoclonal DR5 Ab, an anticancer agent inducing apoptosis of cancer cells by targeting DR5, was physically adsorbed on the surface of HA-modified AuNR via possible hydrophobic and electrostatic interaction.<sup>13,14</sup> The stability of HA-AuNR/DR 5 Ab complex was confirmed by in vitro release test in a bovine serum albumin solution (10 mg/mL) at 37 °C with only 12% of DR5 Ab release from the complex in 48 h. The stable formation of HA-AuNR/DR 5 Ab complex was corroborated by UV–vis spectroscopy, DLS, and TEM. According to UV–vis spectroscopy (Figure 2b), the longitudinal surface plasmon resonance (LSPR) peak of AuNR appeared at 818 nm and transverse surface plasmon resonance (TSPR) at 518 nm, indicating the successful synthesis of rod-shaped AuNPs. After stepwise binding of HA-SH and DR5 Ab on the surface of AuNR, the LSPR peaks were red-shifted to 825 and 826 nm, respectively. The results revealed that HA-SH and DR5 Ab were successfully attached to AuNRs.

We also measured the hydrodynamic size and the zeta potential of AuNR, HA-AuNR, and HA-AuNR/DR5 Ab complex by DLS (Figure 3a). The hydrodynamic size of AuNR was ca. 2.33 and 37.84 nm (transverse size and longitudinal size), that of HA-AuNR was ca. 18.17 and 141.80

nm, and that of HA-AuNR/DR5 Ab complex was ca. 15.69 and 91.28 nm, respectively (Figure 3a). The smaller particle size of HA-AuNR/DR5 Ab complex compared to that of HA-AuNR might be explained by the electrostatic interaction between the positively charged DR5 Ab (isoelectric point = 7.28) and the long, linear, and negatively charged HA chains (isoelectric point = 2.5)<sup>33</sup> on the surface of AuNR. The zeta potential of AuNR, HA-AuNR, and HA-AuNR/DR5 Ab complex were  $19.37 \pm 4.56$ ,  $-16.67 \pm 0.85$ , and  $-4.20 \pm 1.20$  mV, respectively (Figure 3b). Considering HA-SH chain has a negative charge and DR5 Ab has a positive charge in phosphate-buffered saline (PBS), the results directly prove the successful formation of HA-AuNR and HA-AuNR/DR5 Ab complex. Besides, TEM clearly showed the morphology of HA-AuNR (Figure 3c) and HA-AuNR/DR5 Ab complex (Figure 3d). Remarkably, a thin layer of DR5 Ab surrounding AuNR was observed for the case of HA-AuNR/DR5 Ab complex. Furthermore, we measured the number of HA and DR5 Ab bound to a single AuNR. The concentration of AuNR was determined by inductively coupled plasma (ICP) analysis (0.112 nM at the absorbance level of 0.228 in Figure 2b). The concentration of HA and DR5 Ab was determined by measuring the fluorescence of fluorescent dyes labeled on HA and DR5 Ab. From the results, ca. 81.8 of HA and 10.5 of DR5 Ab appeared to be bound to a single AuNR.<sup>13,14</sup>

**In Vitro Biological Activity of HA-AuNR/DR5 Ab Complex.** We assessed the antigen binding of HA-AuNR/DR5 Ab complex to DR5 by ELISA to confirm anticancer effect of the complex (Figure 4). The DR5 (antigen)-coated plate was incubated with various concentrations of DR5 Ab or HA-AuNR/DR5 Ab complex ranging from 0.0137 to 10  $\mu$ g/mL of

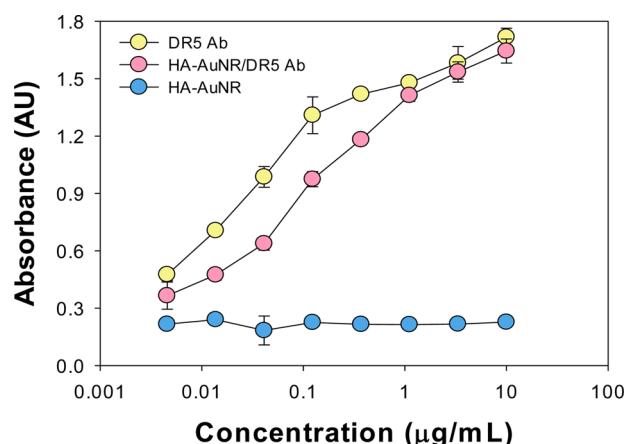


**Figure 4.** ELISA for the binding of HA-AuNR as a control, DR5 Ab, and HA-AuNR/DR5 Ab complex to DR5 ( $n = 3$ ).

DR5 Ab using HA-AuNR as a control. After the plate was washed to remove unbound DR5 and the complex, antihuman IgG-horse radish peroxidase (HRP) was treated to the plate for detecting DR5 Ab bound to DR5. As expected, because DR5 Ab was physically bound to HA-AuNR, there was no significant difference in the antigen binding capability between DR5 Ab alone and HA-AuNR/DR5 Ab complex. Besides, *in vitro* anticancer effect of HA-AuNR/DR5 Ab complex was assessed in a human colon cancer cell line of HCT116 (Figure 5). In

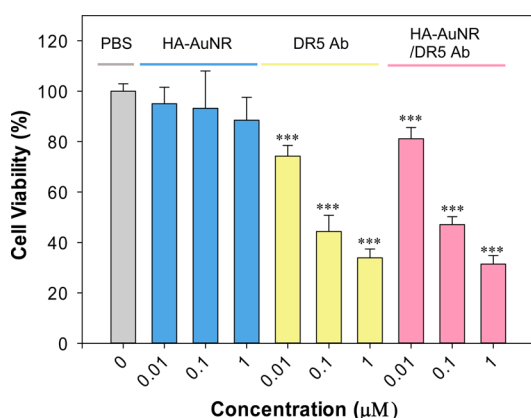


**Figure 5.** Cytotoxicity of PBS as a control, HA-AuNR, DR5 Ab, and HA-AuNR/DR5 Ab complex in HCT116 cancer cells. Samples were treated at the concentration of 0.01, 0.1, and 1  $\mu\text{M}$  of DR5 Ab. The values of  $*P < 0.05$  in comparison with the PBS-treated group were considered to be statistically significant ( $n = 5$ ).

*in vitro* cytotoxicity of HA-AuNR/DR5 Ab complex was dose-dependently comparable to that of DR5 Ab alone in HCT116 cancer cells. On the other hand, there was no significant cytotoxicity for the case of HA-AuNR alone. From the results, we could confirm the biological activity of HA-AuNR/DR5 Ab complex for the treatment of cancers.

**In Vivo Bioimaging for Transdermal Delivery of HA-AuNR/DR5 Ab Complex.** As shown in Figure 6, photoacoustic imaging clearly visualized the effective transdermal delivery of HA-AuNR/DR5 Ab complex, penetrating through the skin barrier significantly compared to DR5 Ab alone. AuNR in the complex inside the back skin of mice was clearly observed on the photoacoustic images at 800 nm. Because AuNR has strong and narrow LSPR peaks in the NIR region

(Figure 2b), photoacoustic microscopy can easily detect AuNR without any pretreatment even inside the deep skin tissue of mice. The result clearly supports the role of HA-AuNR as a skin penetration enhancer and bioimaging agent. To make it clearer, DR5 Ab was labeled with a fluorescent dye and visualized by two-photon microscopy after topical delivery onto mouse back skin (Figure 7). For the case of DR5 Ab alone, just a little fluorescence signal was detected only on the very outer skin layer. However, in the case of HA-AuNR/DR5 Ab complex, we could observe highly significant fluorescent signals within both epidermis and dermis areas together with the blue autofluorescence of collagen, a structural component of dermis. Furthermore, considering the quenching effect of fluorescent dye on AuNR,<sup>34</sup> the observed fluorescence indicates the rapid release of DR5 Ab from HA-AuNR/DR5 Ab complex in the skin tissue. All these bioimaging results clearly confirm the successful transdermal delivery of HA-AuNR/DR5 Ab complex.

**In Vivo Antitumor Effect of HA-AuNR/DR5 Ab Complex.** Skin cancer model mice were prepared by inoculating luciferase-expressing HCT116 cancer cells in the dorsal flank of balb/c nude mice. After a week, mice were treated with four types of samples: PBS, HA-AuNR, DR5 Ab, and HA-AuNR/DR5 Ab complex. The progress of cancer was monitored using IVIS after peritoneal injection of luciferin which reacts with luciferase of HCT116 cancer cells producing bioluminescence. Figure 8 shows the progress of cancer monitored by IVIS for the fluorescence intensity of cancer tissues after treatment with the samples for 5 days. There were little differences among the groups treated with PBS, HA-AuNR, and DR5 Ab, showing dramatic cancer growth due to the negligible antitumor effect of HA-AuNR and the poor skin penetration of DR5 Ab. In contrast, HA-AuNR/DR5 Ab complex resulted in drastically reduced tumor growth for up to 5 days, which was certainly distinguishable from the other groups.

After bioimaging with IVIS, cancer tissues treated with PBS, HA-AuNR, DR5 Ab, and HA-AuNR/DR5 Ab complex were harvested and sectioned for histological analysis to investigate the apoptosis of cancer cells by fluorescence TUNEL assay (Figure 9). Cancer cell nuclei were stained in blue and the TUNEL-positive cells reflecting apoptosis were stained in green. Only a few and sparsely spread green signals were observed in the groups treated with PBS (Figure 9a), HA-AuNR (Figure 9b), and DR5 Ab (Figure 9c). However, green signals were clearly observed in almost the entire area of cancer tissues treated with HA-AuNR/DR5 Ab complex (Figure 9d), which explicitly proved the effective skin penetration and anticancer effect of the HA-AuNR/DR5 Ab complex.

## CONCLUSION

We have developed HA-AuNR/DR5 Ab complex as a theranostic platform for noninvasive transdermal treatment of skin cancers. After *in vitro* characterization by  $^1\text{H}$  NMR, UV-vis spectroscopy, DLS, TEM, ELISA, and MTT assay, *in vivo* transdermal delivery and antitumor effect of HA-AuNR/DR5 Ab complex in skin cancer model mice were confirmed by photoacoustic imaging, two-photon microscopy, *in vivo* fluorescence imaging with IVIS, and TUNEL assay. The transdermally delivered HA-AuNR/DR5 Ab complex resulted in drastically reduced tumor growth for up to 5 days. The theranostic HA-AuNR/antibody complex might be successfully exploited as a new platform for noninvasive transdermal treatment of various diseases in the skin. On the basis of this

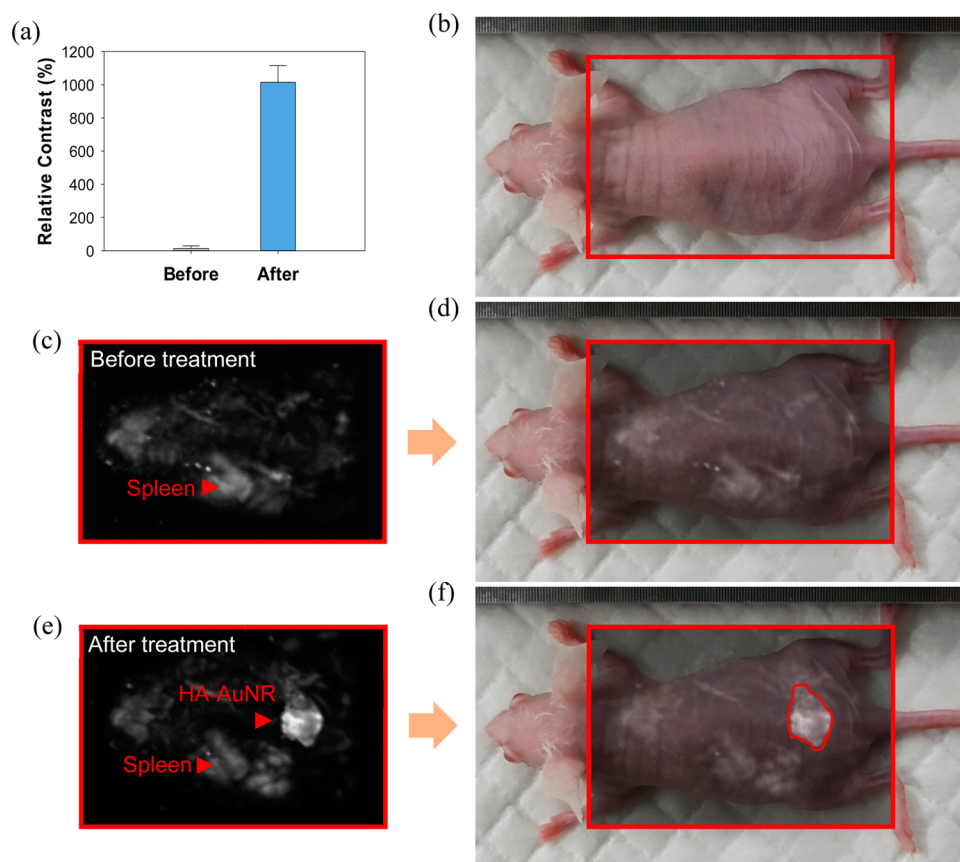


**Figure 6.** Photoacoustic (PA) microscopy for transdermal delivery of HA-AuNR through mouse back skin at 800 nm wavelength. (a) Relative contrast (%) of PA signals before and after the transdermal delivery. (b) Photograph of mouse as an untreated control group. PA images of mice (c, d) before and (e, f) after treatment with HA-AuNR.

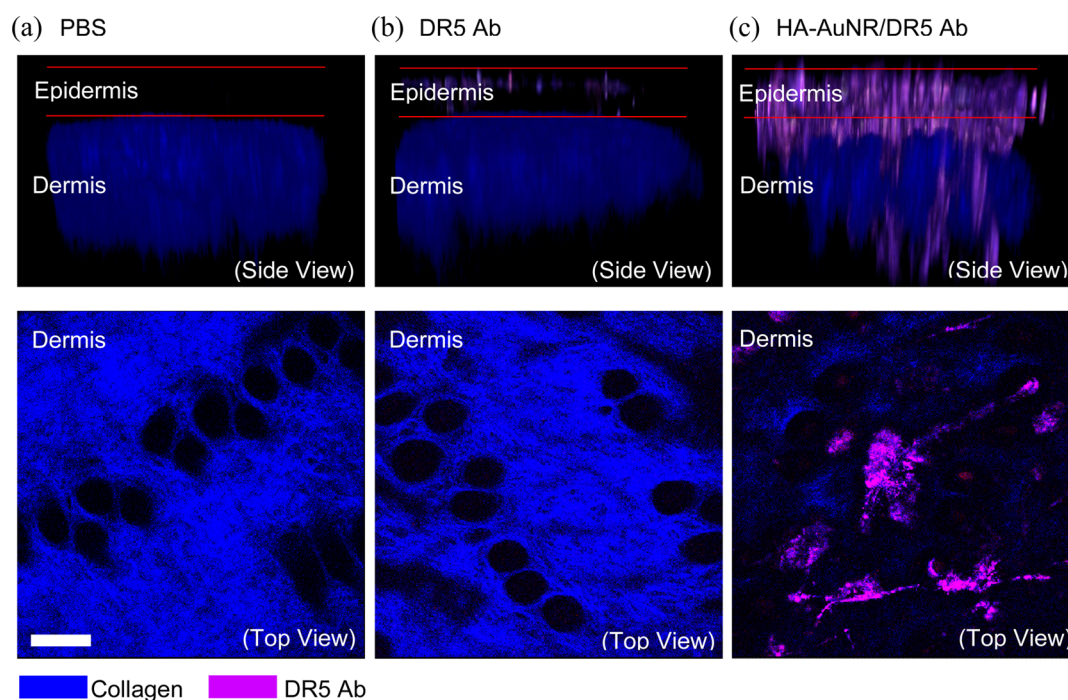


**Figure 7.** Two-photon microscopic images of back skin in mice after treatment with (a) PBS, (b) DR5 Ab, and (c) HA-AuNR/DR5 Ab complex. The blue color (autofluorescence) reflects collagen, a structural component of dermis. The purple color indicates fluorescent dye labeled DR5 Ab (scale bar = 50  $\mu\text{m}$ ).

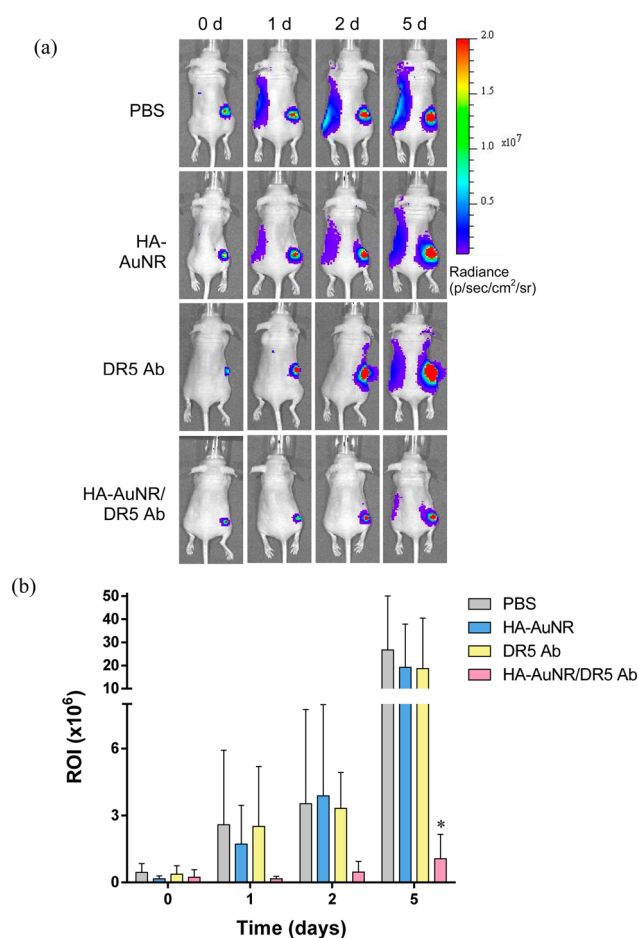


**Figure 8.** In vivo bioimaging of luciferase-expressing HCT116 cancer cells inoculated into the back skin of mice for 5 days, which reflects anticancer effect of the treatment with PBS, HA-AuNR, DR5 Ab, and HA-AuNR/DR5 Ab complex. (a) IVIS images and (b) the average level of luciferase ROI values of skin cancers in the right dorsal flank of mice. The value of \* $P < 0.05$  compared to the PBS-treated group was considered to be statistically significant ( $n = 5$ ).

proof-of-concept study, the detailed theranostic assessment of HA-AuNR/DR5 Ab complex will be followed for further applications.

## MATERIALS AND METHODS

**Materials.** Ascorbic acid, chloroauric acid ( $\text{HAuCl}_4$ ), silver nitrate, sodium borohydride, cetrionium bromide (CTAB), sodium cyanoborohydride, DL-dithiothreitol (DTT), and acetic acid were obtained from Sigma-Aldrich (St. Louis). Sodium hyaluronate (HA) with a molecular weight of 10 kDa was purchased from Lifecore Co. (Chaska, MN). Cystamine dihydrochloride was obtained from Tokyo Chemical Industry (Tokyo, Japan). Tris(2-carboxyethyl)phosphine hydrochloride (TCEP) was purchased from Alfa Aesar (Haverhill, MA). PD-10 column and NAP-5 desalting column were obtained from GE Healthcare (Chicago, IL). Deuterium oxide ( $\text{D}_2\text{O}$ ) was obtained from Cambridge Isotope Laboratories Inc. (Cambridge, MA). PVDF syringe filter (0.45  $\mu\text{m}$ ) and centrifugal filter (MWCO = 10 kDa) were purchased from Merck Millipore (Billerica, MA). HiLyte 647 amine was purchased from AnaSpec Inc. (Fremont, CA). HCT 116 cells were purchased from PerkinElmer (Waltham, MA). RPMI 1640 was obtained from MediaTek Inc. (Hsinchu City, Taiwan). FBS, antibiotics, and Alexa Fluor 532 NHS ester were purchased from Thermo Fisher Scientific (Waltham, MA). MTT solution was obtained from Georgia Tech Chemistry & Biochemistry (Atlanta, GA). Luciferin was purchased from SIhealthcare (Seoul, Korea). DeadEnd

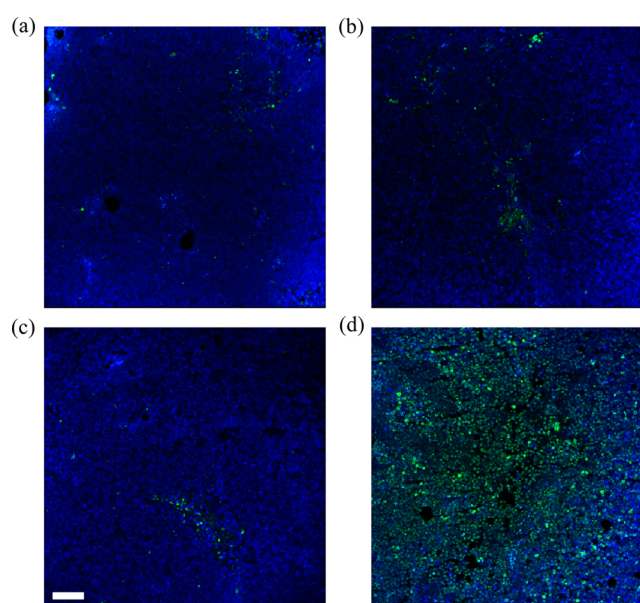


**Figure 9.** Histological TUNEL assay of skin cancer tissues harvested and sectioned after treatment with (a) PBS, (b) HA-AuNR, (c) DR5 Ab, and (d) HA-AuNR/DR5 Ab complex. The blue signal shows cancer cell nuclei stained with DAPI and the green signal indicates apoptotic cancer cells (scale bar = 50  $\mu\text{m}$ ).

fluorometric TUNEL assay kit was purchased from Promega (Fitchburg, WI).

**Synthesis of End-Thiolated HA.** End-group modified HA-SH was synthesized by reductive amidation.<sup>13,14</sup> HA (MW 10 kDa, 10 mg) and cystamine dihydrochloride (6 mg) were dissolved in 2 mL of borate buffer (0.1 M, pH 8.5) containing 0.4 M sodium chloride for 2 h. Then sodium cyanoborohydride (200 mM) was added to the mixed solution and incubated at 40 °C for 5 days. To reduce disulfide bonds of cystamine at the end of HA chain, 100 mM DTT was added to the reaction mixture, which was mixed for 12 h. The solution was repeatedly dialyzed against 5 L of sodium chloride solution (100 mM), 25% ethanol, and distilled water for a day, respectively, and freeze-dried for 2 days. Before use, end-thiolated HA was treated with TCEP to completely reduce disulfide bonds and purified with a PD-10 desalting column. The reduced free thiol group at the end of HA chains in deuterium oxide was analyzed by <sup>1</sup>H NMR and Ellman's assay.

**Synthesis of AuNR.** Both a seed solution and a growth solution were mixed for the seed-mediated growth of AuNR. The seed solution was prepared by mixing CTAB (72.89 mg/mL, 5 mL),  $\text{HAuCl}_4$  (0.1968 mg/mL, 5 mL), and freshly prepared ice-cold sodium borohydride solution (0.3767 mg/mL, 0.6 mL) at 37 °C for 2 h. The color of the solution changed from yellow to brown upon vigorous stirring. The growth solution was prepared by mixing CTAB (72.89 mg/mL, 50 mL) with silver nitrate (0.6793 mg/mL, 5 mL) and  $\text{HAuCl}_4$  (0.5513 mg/mL, 50 mL) aqueous solutions at 37 °C. After gentle mixing, ascorbic solution (17.61 mg/mL, 0.55 mL) was added, which changed the solution color to transparent. Then the seed solution (0.12 mL) was added to the growth solution, which was incubated for 24 h. After that, excess CTAB was removed by centrifugation (13000g, 10 min, 20 °C) and redispersion in distilled water twice.

**Preparation of HA-AuNR/DR5 Ab Complex.** End-thiolated HA (10 mg/mL, 0.1 mL) was added to 20 mL of AuNR in the presence of sodium chloride (2.338 mg/mL, 1 mL) to prevent the AuNR aggregation. The solution was mixed at room temperature for 6 h. HA-AuNR was purified by centrifugation (13000g, 10 min, 20 °C) and redispersed in 20 mL of PBS. Then DR5 Ab in PBS (0.1 mg/mL, 6 mL) was slowly added to HA-AuNR, which was incubated at room temperature for 4 h to prepare HA-AuNR/DR5 Ab complex. The

unbound DR5 Ab was purified by centrifugation and redispersion in PBS. The solution was filtered with a PVDF syringe filter (0.45  $\mu\text{m}$ ) for the following experiments.

**In Vitro Biological Activity of HA-AuNR/DR5 Ab Complex.** In vitro specific binding of HA-AuNR/DR5 Ab complex to DR5 was assessed by ELISA. First, DR5 (2 ng/mL) in sodium carbonate buffer (pH 9) was coated on a 96-well plate with a plate sealer by incubating at 4 °C overnight. After the plate was washed with TTBS buffer four times, the wells were incubated with a blocking buffer (1% skim milk in pH 9 carbonate buffer) at room temperature for 2 h. Then DR5 Ab and HA-AuNR/DR5 Ab complex in the range from 0.0137 to 10  $\mu\text{g}/\text{mL}$  were incubated in the DR5-coated wells at room temperature with mild shaking for 2 h. After they were washed with TTBS buffer four times, goat antihuman IgG-horseradish peroxidase (HRP), which specifically binds to DR5 Ab, was added and incubated with mild shaking for 2 h. Finally, 50  $\mu\text{L}$  of TMB solution prepared by mixing TMB (6 mg/mL, 100  $\mu\text{L}$ ) in DMSO and  $\text{H}_2\text{O}_2$  (30%, 0.6  $\mu\text{L}$ ) in acetic acid (100 mM, pH 5.5, 6 mL) was added to each well to activate the HRP in the dark for 20 min. Then the stop solution prepared by diluting 533  $\mu\text{L}$  of sulfuric acid (1 M) in 10 mL of distilled water was added in each well to stop the reaction. The absorbance of each well was measured at 450 nm with a microplate reader (EMax, Molecular Devices, Sunnyvale, CA).

**In Vitro Antitumor Effect of HA-AuNR/DR5 Ab Complex.** A human colon cancer cell line of HCT116 was seeded on 96-well plates at a density of  $2 \times 10^4$  cells per well and cultured in RPMI 1640 containing 10 vol % FBS and 1 vol % antibiotics at 37 °C and 5%  $\text{CO}_2$  atmosphere for a day. After that, HCT116 cells in 100  $\mu\text{L}$  of serum-free RPMI 1640 were incubated with PBS, HA-AuNR, DR5 Ab, or HA-AuNR/DR5 Ab complex at the concentration of 0.01, 0.1, and 1  $\mu\text{M}$  of DR5 Ab for 24 h. Then the sample containing media in each well were removed by gentle suction and 100  $\mu\text{L}$  of fresh serum-free media containing 10  $\mu\text{L}$  of MTT solution (5 mg/mL) was added to the wells. After incubation at 37 °C and 5%  $\text{CO}_2$  atmosphere for 2 h, the plate was cleaned by gentle suction and treated with 50  $\mu\text{L}$  of DMSO in each well. The optical density of each well was measured with a microplate reader at 540 nm to determine the antitumor effect of HA-AuNR/DR5 Ab complex.

**In Vivo Bioimaging of HA-AuNR/DR5 Ab Complex.** The transdermal delivery of HA-AuNR/DR5 Ab complex was investigated by photoacoustic imaging and two-photon microscopy. Photoacoustic images of BALB/c nude mice were acquired after topical treatment of HA-AuNR (50 nM) for 1 h and subsequent washing. A Q-switched Nd:YAG laser (Surelite III-10, Continuum, Boston, MA) and a tunable optical parametric oscillator (OPO) laser (Surelite OPO PLUS, Continuum, Boston, MA) were used to excite the photoacoustic signals. By tuning the OPO laser, a short laser pulse with a wavelength of 800 nm was illuminated to the target tissues. The generated photoacoustic waves were acquired by the spherically focused ultrasound transducer (V308, Olympus NDT, Center Valley, PA) with a focal length of 25 mm and a center frequency of 5 MHz. Then the photoacoustic signals were amplified by an amplifier (5072PR, Olympus NDT, Center Valley, PA) with a gain of 35 dB and digitized by the data acquisition system (MSO5204, Tektronix, Beaverton, OR) with a sampling frequency of 40 MHz. To obtain volumetric photoacoustic images from a whole body of a mouse, mechanical raster scanning was performed with a field of view of  $60 \times 40$  mm along X and Y directions, respectively. The scanning step size was 0.2 and 0.4 mm in X and Y directions, respectively. The whole body photoacoustic images were reconstructed using a maximum amplitude projection method.<sup>35–38</sup>

In addition, the transdermal delivery of HA-AuNR/DR5 Ab complex was visualized by two-photon microscopy (Leica TCS SP5). An amino-reactive form of fluorescence dye (Alexa Fluor 532 NHS ester, Ex/Em = 530/555 nm) was attached to amine groups of DR5 Ab. In detail, 10 molar ratio of dye was reacted with DR5 Ab at room temperature in dark overnight and then purified with a centrifugal filter (MWCO = 10 kDa, 10000g, 10 min) and a NAP-5 desalting column (GE Healthcare, UK) to remove the unbound fluorescence dye. Three types of samples (20  $\mu\text{L}$ ) including PBS, DR5

Ab, and HA-AuNR/DR5 Ab complex with the same fluorescent intensity were applied on the back skin of mice. After 1 h, the mice were sacrificed and the back skin tissues were harvested for two-photon microscopy.

**In Vivo Antitumor Effect of HA-AuNR/DR5 Ab Complex.** Skin cancer model mice were prepared by the inoculation of luciferase-expressing HCT116 cancer cells at a density of  $3.5 \times 10^6$  in the right flank of 7-week-old male BALB/c (nu/nu) mice (Orient Bio Inc., Korea). Although the HCT116 cell is originated from the colon tissue, it has been used for the preparation of the skin cancer models,<sup>39</sup> especially showing the high sensitivity to DR5 Ab.<sup>40</sup> The skin cancer model mice ( $n = 5$ ) were treated with four types of samples: PBS, HA-AuNR, DR5 Ab, and HA-AuNR/DR5 complex. The final volume of each sample was 20  $\mu\text{L}$  for each mouse containing an equal amount of DR5 Ab or HA-AuNR in PBS. Under anesthesia, the sample solution was topically delivered onto the cancerous skin of mice for 1 h. The tumor growth was monitored for 5 days by measuring luciferase intensity using the IVIS system after peritoneal luciferin (SIhealthcare, Korea) injection (15 mg/mL, 0.1 mL). All animal experimental procedures were performed in accordance with protocols approved by an institutional animal care and use committee of Pohang University of Science and Technology (POSTECH).

**Histological Analysis of Cancer Apoptosis.** After monitoring for the progress of skin cancer using the IVIS system, cancer tissues treated with PBS, HA-AuNR, DR5 Ab, and HA-AuNR/DR5 Ab complex were harvested for histological apoptosis analysis. All harvested skin cancer tissues were washed with PBS and fixed in 10% (v/v) buffered formalin for storage. The fixed skin cancer tissues were washed with distilled water, dehydrated by simple immersion in a graded ethanol series (70%, 80%, 95%, 100%) several times, and embedded in paraffin. The paraffin-embedded liver tissues were sliced into 4  $\mu\text{m}$  thick for TUNEL assay. The fluorometric TUNEL assay shows apoptotic cancer cells by catalytically incorporating fluorescein-12-dUTP at 3'-OH DNA ends using the terminal deoxynucleotidyl transferase.<sup>25</sup> The fragmented DNA of apoptotic cancer cells labeled with fluorescein-12-dUTP was observed with a confocal microscope (Leica TCS SP5, Deerfield, IL).

## AUTHOR INFORMATION

### Corresponding Author

\*Tel.: +82 54 279 2159. Fax: +82 54 279 2399. E-mail: skhanb@postech.ac.kr (S.K.H.).

### ORCID

Sei Kwang Hahn: 0000-0002-7718-6259

### Author Contributions

<sup>#</sup>These authors contributed equally to this work.

### Notes

The authors declare no competing financial interest.

## ACKNOWLEDGMENTS

This research was supported by the Bio & Medical Technology Development Program (No. 2012M3A9C6049791) and Midcareer Researcher Program (No. 2015R1A2A1A15053779) of the National Research Foundation (NRF) funded by the Korean government (MEST). This work was supported by Korea Health Technology R&D Project (HI15C1817) of the Ministry of Health and Welfare.

## REFERENCES

- (1) Vigderman, L.; Zubarev, E. R. Therapeutic Platforms Based on Gold Nanoparticles and Their Covalent Conjugates with Drug Molecules. *Adv. Drug Delivery Rev.* **2013**, *65* (5), 663–676.
- (2) Harris, N.; Arnold, M. D.; Blaber, M. G.; Ford, M. J. Plasmonic Resonances of Closely Coupled Gold Nanosphere Chains. *J. Phys. Chem. C* **2009**, *113* (7), 2784–2791.

- (3) Brioude, A.; Jiang, X. C.; Pileni, M. P. Optical Properties of Gold Nanorods: DDA Simulations Supported by Experiments. *J. Phys. Chem. B* **2005**, *109* (27), 13138–13142.
- (4) Zhou, X.; Li, H.; Fu, S.; Xie, S.; Xu, H.; Wu, J. Optical Properties and Plasmon Resonance of Coupled Gold Nanoshell Arrays. *Mod. Phys. Lett. B* **2011**, *25* (2), 109–118.
- (5) Chen, J.; Saeki, F.; Wiley, B. J.; Cang, H.; Cobb, M. J.; Li, Z.-Y.; Au, L.; Zhang, H.; Kimmey, M. B.; Xingde; Xia, Y. Gold Nanocages: Bioconjugation and Their Potential Use as Optical Imaging Contrast Agents. *Nano Lett.* **2005**, *5* (3), 473–477.
- (6) Manohar, S.; Unquareanu, C.; Van Leeuwen, T. G. Gold Nanorods as Molecular Contrast Agents in Photoacoustic Imaging: the Promises and the Caveats. *Contrast Media Mol. Imaging* **2011**, *6* (5), 389–400.
- (7) Kim, C.; Cho, E. C.; Chen, J.; Song, K. H.; Au, L.; Favazza, C.; Zhang, Q.; Cogley, C. M.; Gao, F.; Xia, Y.; Wang, L. V. *In Vivo* Molecular Photoacoustic Tomography of Melanomas Targeted by Bio-Conjugated Gold Nanocages. *ACS Nano* **2010**, *4* (8), 4559–4564.
- (8) Jain, S.; Hirst, D. G.; O'Sullivan, J. M. Gold Nanoparticles as Novel Agents for Cancer Therapy. *Br. J. Radiol.* **2012**, *85* (1010), 101–113.
- (9) Huang, X.; El-Sayed, I. H.; Qian, W.; El-Sayed, M. A. Cancer Cell Imaging and Photothermal Therapy in the Near-Infrared Region by Using Gold Nanorods. *J. Am. Chem. Soc.* **2006**, *128* (6), 2115–2120.
- (10) Liu, L.; Ouyang, S.; Ye, J. Gold-Nanorod-Photosensitized Titanium Dioxide with Wide-Range Visible-Light Harvesting Based on Localized Surface Plasmon Resonance. *Angew. Chem., Int. Ed.* **2013**, *52* (26), 6689–6693.
- (11) Mohammed, M. A.; Dobliger, M.; Rodriguez-Fernandez, J. Switching Plasmons: Gold Nanorod-Copper Chalcogenide Core-Shell Nanoparticle Clusters with Selectable Metal/Semiconductor NIR Plasmon Resonances. *J. Am. Chem. Soc.* **2015**, *137* (36), 11666–11677.
- (12) Arimoto, H.; Egawa, M. Imaging Wavelength and Light Penetration Depth for Water Content Distribution Measurement of Skin. *Skin Res. Technol.* **2015**, *21* (1), 94–100.
- (13) Lee, M.; Yang, J.; Jung, H. S.; Beack, S.; Choi, J. E.; Hur, W.; Koo, H.; Kim, K.; Yoon, S. K.; Hahn, S. K. Hyaluronic Acid-Gold Nanoparticle/Interferon  $\alpha$  Complex for Targeted Treatment of Hepatitis C Virus Infection. *ACS Nano* **2012**, *6* (11), 9522–9531.
- (14) Lee, H.; Lee, M.; Bhang, S. H.; Kim, B.; Kim, Y. S.; Ju, J. H.; Kim, K. S.; Hahn, S. K. Hyaluronate-Gold Nanoparticle/Tocilizumab Complex for the Treatment of Rheumatoid Arthritis. *ACS Nano* **2014**, *8* (5), 4790–4798.
- (15) Jazayeri, M. H.; Amani, H.; Pourfatollah, A. A.; Pazoki-Toroudi, H.; Sedighimoghaddam, B. Various Methods of Gold Nanoparticles (GNPs) Conjugation to Antibodies. *Sens. Biosensing Res.* **2016**, *9*, 17–22.
- (16) Locatelli, E.; Monaco, I.; Franchini, M. C. Surface Modifications of Gold Nanorods for Applications in Nanomedicine. *RSC Adv.* **2015**, *5* (28), 21681–21699.
- (17) Yu, C.; Varghese, L.; Irudayaraj, J. Surface Modification of Cetyltrimethylammonium Bromide-Capped Gold Nanorods to Make Molecular Probes. *Langmuir* **2007**, *23* (17), 9114–9119.
- (18) Ma, Z.; Xia, H.; Liu, Y.; Liu, B.; Chen, W.; Zhao, Y. Applications of Gold Nanorods in Biomedical Imaging and Related Fields. *Chin. Sci. Bull.* **2013**, *58*, 2530–2536.
- (19) Liu, Y.; Yang, M.; Zhang, J.; Zhi, X.; Li, C.; Zhang, C.; Pan, F.; Wang, K.; Yang, Y.; de la Fuentea, J. M.; Cui, D. Human Induced Pluripotent Stem Cells for Tumor Targeted Delivery of Gold Nanorods and Enhanced Photothermal Therapy. *ACS Nano* **2016**, *10* (2), 2375–2385.
- (20) Raeesi, V.; Chou, L. Y.; Chan, W. C. Tuning the Drug Loading and Release of DNA-Assembled Gold-Nanorod Superstructures. *Adv. Mater.* **2016**, *28*, 8511–8518.
- (21) Prausnitz, M. R.; Langer, R. Transdermal Drug Delivery. *Nat. Biotechnol.* **2008**, *26*, 1261–1268.
- (22) Toole, B. P. Hyaluronan: from Extracellular Glue to Pericellular Cue. *Nat. Rev. Cancer* **2004**, *4* (7), 528–539.
- (23) Kim, K. S.; Kim, H.; Park, Y.; Kong, W. H.; Lee, S. W.; Kwok, S. J. J.; Hahn, S. K.; Yun, S. H. Noninvasive Transdermal Vaccination Using Hyaluronan Nanocarriers and Laser Adjuvant. *Adv. Funct. Mater.* **2016**, *26*, 2512–2522.
- (24) Yang, J. A.; Kim, E. S.; Kwon, J. H.; Kim, H. M.; Shin, J. H.; Yun, S. H.; Choi, K. Y.; Hahn, S. K. Transdermal Delivery of Hyaluronic Acid - Human Growth Hormone Conjugate. *Biomaterials* **2012**, *33* (25), 5947–5954.
- (25) Jung, H. S.; Kong, W. H.; Sung, D. K.; Lee, M. Y.; Beack, S. E.; Keum, D. H.; Kim, K. S.; Yun, S. H.; Hahn, S. K. Nanographene Oxide-Hyaluronic Acid Conjugate for Photothermal Ablation Therapy of Skin Cancer. *ACS Nano* **2014**, *8* (1), 260–268.
- (26) Brown, M. B.; Jones, S. A. Hyaluronic Acid: A Unique Topical Vehicle for the Localized Delivery of Drugs to the Skin. *J. Eur. Acad. Dermatol. Venereol.* **2005**, *19* (3), 308–318.
- (27) Papakonstantinou, E.; Roth, M.; Karakiulakis, G. Hyaluronic Acid: A Key Molecule in Skin Aging. *Derm.-Endocrinol.* **2012**, *4* (3), 253–258.
- (28) Ichikawa, K.; Liu, W.; Zhao, L.; Wang, Z.; Liu, D.; Ohtsuka, T.; Zhang, H.; Mountz, J. D.; Koopman, W. J.; Kimberly, R. P.; Zhou, T. Tumorocidal Activity of a Novel Anti-Human DR5 Monoclonal Antibody without Hepatocyte Cytotoxicity. *Nat. Med.* **2001**, *7* (8), 954–960.
- (29) Graves, J. D.; Kordich, J. J.; Huang, T. H.; Piasecki, J.; Bush, T. L.; Sullivan, T.; Foltz, I. N.; Chang, W.; Douangpanya, H.; Dang, T.; O'Neill, J. W.; Mallari, R.; Zhao, X.; Branstetter, D. G.; Rossi, J. M.; Long, A. M.; Huang, X.; Holland, P. M. Apo2L/TRAIL and the Death Receptor 5 Agonist Antibody AMG 655 Cooperate to Promote Receptor Clustering and Antitumor Activity. *Cancer Cell* **2014**, *26*, 177–189.
- (30) Bullen, C.; Zijlstra, P.; Bakker, E.; Gu, M.; Raston, C. Chemical Kinetics of Gold Nanorod Growth in Aqueous CTAB Solutions. *Cryst. Growth Des.* **2011**, *11* (8), 3375–3380.
- (31) Rouhana, L. L.; Moussallem, M. D.; Schlenoff, J. B. Adsorption of Short-Chain Thiols and Disulfides onto Gold under Defined Mass Transport Conditions: Coverage, Kinetics, and Mechanism. *J. Am. Chem. Soc.* **2011**, *133* (40), 16080–16091.
- (32) Sonavane, G.; Tomoda, K.; Sano, A.; Ohshima, H.; Terada, H.; Makino, K. In Vitro Permeation of Gold Nanoparticles Through Rat Skin and Rat Intestine: Effect of Particle Size. *Colloids Surf., B* **2008**, *65*, 1–10.
- (33) Stern, R.; Asari, A. A.; Sugahara, K. N. Hyaluronan Fragments: An Information-Rich System. *Eur. J. Cell Biol.* **2006**, *85*, 699–715.
- (34) Dulkeith, E.; Morteaux, A. C.; Niedereichholz, T.; Klar, T. A.; Feldmann, J.; Levi, S. A.; van Veggel, F. C. J. M.; Reinhoudt, D. N.; Möller, M.; Gittins, D. I. Fluorescence Quenching of Dye Molecules near Gold Nanoparticles: Radiative and Nonradiative Effects. *Phys. Rev. Lett.* **2002**, *89* (20), 203002.
- (35) Jeon, M.; Kim, J.; Kim, C. Multiplane Spectroscopic Whole-Body Photoacoustic Imaging of Small Animals. *Med. Biol. Eng. Comput.* **2016**, *54*, 283–294.
- (36) Kim, C.; Favazza, C.; Wang, L. V. *In Vivo* Photoacoustic Tomography of Chemicals: High-Resolution Functional and Molecular Optical Imaging at New Depths. *Chem. Rev.* **2010**, *110*, 2756–2782.
- (37) Lee, M. Y.; Lee, C.; Jung, H. S.; Jeon, M.; Kim, K. S.; Yun, S. H.; Kim, C.; Hahn, S. K. Biodegradable Photonic Melanoidin for Theranostic Applications. *ACS Nano* **2016**, *10* (1), 822–831.
- (38) Zhang, Y.; Jeon, M.; Rich, L. J.; Hong, H.; Geng, J.; Zhang, Y.; Shi, S.; Barnhart, T. E.; Alexandridis, P.; Huizinga, J. D.; Seshadri, M.; Cai, W.; Kim, C.; Lovell, J. F. Non-Invasive Multimodal Functional Imaging of the Intestine with Frozen Micellar Naphthalocyanines. *Nat. Nanotechnol.* **2014**, *9*, 631–638.
- (39) Pukac, L.; Kanakaraj, P.; Humphreys, R.; Alderson, R.; Bloom, M.; Sung, C.; Riccobene, T.; Johnson, R.; Fiscella, M.; Mahoney, A.; Carrell, J.; Boyd, E.; Yao, X. T.; Zhang, L.; Zhong, L.; von Kerczek, A.; Shepard, L.; Vaughan, T.; Edwards, B.; Dobson, C.; Salcedo, T.; Albert, V. HGS-ETRI, A Fully Human TRAIL-receptor 1 Monoclonal

Antibody, Induces Cell Death in Multiple Tumour Types In Vitro and In Vivo. *Br. J. Cancer* **2005**, *92* (8), 1430–1441.

(40) Oliver, P. G.; LoBuglio, A. F.; Zinn, K. R.; Kim, H.; Nan, L.; Zhou, T.; Wang, W.; Buchsbaum, D. Treatment of Human Colon Cancer Xenografts with TRA-8 Anti-death Receptor 5 Antibody Alone or in Combination with CPT-11. *Clin. Cancer Res.* **2008**, *14*, 2180–2189.